Sustainable Energy Technologies and Assessments 93 (2026) 105351

Contents lists available at ScienceDirect

Sustainable Energy Technologies and Assessments

journal homepage: www.elsevier.com/locate/seta

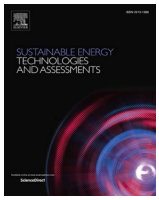

Rapid screening approach to evaluate MEC performance for biohydrogen production using synthetic and real organic waste-derived substrates

Angela Marchetti [a,*], Francesco Valentino [b], Marco Gottardo [b], Marco Zeppilli [a]

[a] Department of Chemistry, Sapienza University of Rome, Piazzale Aldo Moro 5, 00185 Rome, Italy
[b] Department of Environmental Sciences, Informatics and Statistics, "Ca' Foscari" University of Venice, Via Torino 155, 30170 Mestre-Venice City, Italy

ARTICLE INFO

Keywords:
Biohydrogen production
Dual-cathode-chamber
Microbial electrolysis cell
Organic and food waste valorisation
Rapid screening approach

ABSTRACT

In this study, a rapid screening strategy was developed to accelerate the identification of optimal operating conditions in dual-cathode microbial electrolysis cells (MECs) for hydrogen production from synthetic and real waste-derived substrates. The approach consisted of progressively increasing the hydraulic loading while evaluating system performance through current production, $COD_{removal}$ efficiency, hydrogen recovery, and electrochemical efficiencies, enabling rapid identification of operational boundaries and the onset of the performance plateau, guiding the selection of the most fitting operating regime for subsequent steady-state investigations. The real substrate, obtained from dark fermentation of food waste and sewage sludge, exhibited a high organic acid content (82% OA/CODsol) and a low redox potential (≈ −0.278 V vs SHE), confirming its suitability for bioelectrochemical conversion. The dual-cathode configuration achieved complete cathodic electron recovery into hydrogen (CCE ≈ 100%) demonstrating performance improvements, consistent with those expected from enhanced cathodic architecture. Finally, potentiostatic polarization further characterized the electrochemical response of the bioanode. Combined with the proposed screening methodology, these results provide a practical framework for rapidly assessing MEC performance and selecting promising operating conditions before more detailed long-term investigations and scale-up.

1. Introduction

In recent decades, the urgent need to reduce greenhouse gas emissions, mitigating their associated environmental impacts, has driven the energy sector towards increasing interest in renewable materials and clean and energy carriers [1–4]. In line with the European Union's strategic frameworks, including the European Green Deal and its legally binding target of climate neutrality by 2050 [5,6], hydrogen is widely recognizing as a promising energy carrier owing to its high specific energy-to-mass ratio and its potential to generate energy without direct pollutant emissions [7]. Nevertheless, conventional hydrogen production routes, such as steam methane reforming, remain largely dependent on fossil resources and are associated with significant environmental and economic burdens [8,9]. Consequently, growing attention has focused on alternative low-carbon pathways for hydrogen production [10].

Within this context, several bio-based technologies have been explored, including dark-, photo-, and integrated fermentation–electrochemical systems that enable the recovery of hydrogen from fermented-derived substrates [11–15]. Among these approaches, microbial electrolysis cells (MECs) represent a particularly promising platform, due to the exploitation of the metabolic activity of electroactive microorganisms, capable to convert organic matter into electrons and protons, which can be electrochemically recovered into biofuels as hydrogen [16–18]. Compared to conventional water electrolysis, MECs operate under mild conditions and can be directly coupled with waste streams, enabling the simultaneous production of renewable energy carriers, wastewater treatment and waste valorisation, especially when mixed microbial cultures (MMCs) are employed [19–22]. Despite these advantages, the practical deployment of MECs is still constrained by their strong sensitivity to several conditions. System performance is governed by a complex interplay between microbial activity, substrate composition, hydraulic and electrochemical parameters, making MEC operation particularly challenging when complex and heterogeneous real waste streams and derived-substrate are used as feedstock [23–28]. Most published MEC studies focus on the

* Corresponding author.
E-mail addresses: angela.marchetti@uniroma1.it (A. Marchetti), francesco.valentino@unive.it (F. Valentino), marco.gottardo@unive.it (M. Gottardo), marco.zeppilli@uniroma1.it (M. Zeppilli).

https://doi.org/10.1016/j.seta.2026.105351
Received 6 April 2026; Received in revised form 10 July 2026; Accepted 20 August 2026
Available online 24 August 2026

optimization of specific operational or design parameters through extensive long-term experimentation under selected conditions [29–36]. Although these approaches have substantially advanced the field, they are primarily intended to maximize system performance rather than to provide a rapid preliminary assessment capable of efficiently narrowing the operational window before detailed optimization.

In this regard, the development of screening-oriented experimental approaches can represent a valuable diagnostic tool to accelerate MEC optimisation.

In particular, the proposed screening strategy should be viewed as complementary to conventional optimization studies, providing an initial decision-support framework that enables informed selection of the most promising operating conditions for subsequent in-depth investigation, thus avoiding biomass wash-out, microbial stress, or electrochemical imbalance between anodic and cathodic outputs. By progressively varying the hydraulic conditions, and consequently the OLR, while monitoring a limited number of key performance indicators, the approach enables the rapid exclusion of suboptimal operating conditions before undertaking more time-consuming long-term investigations.

Importantly, the rapid nature of the proposed screening does not rely on shortening the stabilization period, but rather on minimizing prolonged experimentation under each condition while efficiently exploring multiple operating points to quickly identify system boundaries, differing from conventional MEC studies where individual conditions are typically investigated over extended periods, often lasting several months [37–39]. Such an approach is particularly relevant for MECs treating real substrates, where extensive trial-and-error optimization are often impractical due to time constraints, system instability, and potential bioanode functionality loss. For this reason, several experimental cases were investigated until the plateau region was reached, using a synthetic substrate, as a benchmark, and a real effluent obtained from the dark fermentation of a mixture of the organic fraction of municipal solid food waste (OFMSW) and sewage sludge.

Further, reactor architecture plays a critical role in determining MEC performance. While most MEC studies rely on single or two-chamber configurations, alternative designs remain largely underexplored. Indeed, three-chamber architecture have been only sporadically investigated under batch conditions, at micro-scale volumes, and often without precise electrochemical control (e.g., absence of a reference electrode and high applied potentials), resulting in limited hydrogen production rates and current densities [40]. From an electrochemical perspective, a dual-cathode configuration is expected to provide several potential advantages over conventional single-cathode designs. By positioning two cathodic compartments on both sides of the bioanode, the average electrode spacing can be reduced, thereby decreasing internal ohmic resistance and the cell potential required to sustain current generation. Moreover, the increased cathodic surface area may enhance electron recovery by providing additional active sites for the hydrogen evolution reaction, potentially improving cathodic coulombic efficiency and overall energy performance. These theoretical advantages provide the rationale for investigating dual-cathode MEC configurations under continuous operation and controlled electrochemical conditions.

In detail, MEC reactor of this study was operated with a three-chamber characterised by an abiotic dual-cathode configuration and a central bioanode, allowing the assessment of how reactor geometry and operating conditions jointly influence current generation, hydrogen recovery, energy efficiency, and $COD_{removal}$ efficiency. By combining a rapid screening methodology with an alternative reactor design, this work provides a framework for the systematic evaluation and optimization of MEC systems, while supporting the development and future scale-up of waste-to-biohydrogen technologies. Consequently, by improving the efficiency of biohydrogen generation from real waste streams and reducing the time required for process optimisation, the proposed approach can contribute to sustainable energy deployment and greenhouse gas mitigation strategies, in line with affordable and clean energy (SDG 7) and climate action (SDG 13) goals.

2. Material and Methods

2.1. Microbial electrolysis cell operating conditions

A laboratory-scale MEC comprised of three identical plexiglas chambers, each with a volume of 0.86 L and internal dimensions of 17 cm × 17 cm × 3 cm, was used for this study. A CMI International cation exchange membrane (CEM) (Membrane International, USA) was installed between the bioanode and the cathodic chambers, sealed with butyl rubber gaskets, permitting the migration of cations. The cathode chambers consisted of two sheets of 316 stainless steel (RS components), each with a surface area of 176.46 cm^2. A granular graphite with a diameter < 4 mm (Faima srl, Milan) was used as filler for the bioanode. A schematic representation of the MEC reactor is reported in Fig. 1. Notably, the graphite granules worked both as the electrode material and as a biocompatible substrate for microbial biofilm development. The microbial consortium used as inoculum consisted of an activated sludge composed of a MMCs from a full-scale wastewater treatment plant. Before the bioanode inoculation, the sludge was washed down with a mineral medium and aerated, thus removing any residual COD. Mineral medium composition is given in [41,42]. The sludge was composed of 2.2 gVSS/L in terms of volatile suspended solids. A 150 mL volume (32% v/v) was introduced into the anodic chamber, operated in batch configuration for 7 days by using a concentrated spike of the synthetic feeding. After this period, the acclimatization of the inoculum occurred, establishing the biofilm on the anode material surface. Subsequently, the reactor was placed in continuous flow mode through the passage of the anode electrolyte, using at first the synthetic solution and then the real fermented substrate.

The feeding solutions were stored in a tedlar bag and delivered to the reactor via tygon tubes using a peristaltic pump, and a second tedlar bag was employed to collect the anodic effluent. In particular, the carbon composition of the synthetic feeding solution was as follows: 1.25 g COD/L, comprised of: glucose 0.68 g/L, sodium acetate 0.20 g/L, peptone 0.22 g/L, and yeast extract 0.15 g/L plus the same mineral medium used to wash the inoculum, with an overall conductivity of 6.0 mS/cm. This synthetic medium, stated as a suitable feedstock for MEC systems in previous studies [43–45], was used as a benchmark to evaluate system performance before testing the real fermented substrate.

The latter consisted of the acid effluent obtained from the OFMSW and sewage sludge dark fermentation, which was diluted with tap water to approach to the same organic concentration of the synthetic medium. However, the resulting solution exhibited a lower conductivity of 2.0 mS/cm. The composition of this real feeding solution was heterogeneous in terms of volatile fatty acids (C2-C5), hexanoic acid, and ethanol; a detailed table is given in the subsection "2.2 *Real substrate characterization*". Also, the pH of both feeding solutions was maintained at around pH 7.5 through a buffer solution of sodium bicarbonate (10% w/w). The use of buffers species in the feeding solutions was necessary to limit anolyte acidification due to the production of protons during the organic substrate's oxidation. The anodic chamber was operated under continuous flow conditions and the investigated operating conditions emerged from a sequential exploration strategy rather than from predefined experimental cases. Hence, the influent flow rate was progressively doubled, and the exploration was stopped once a performance plateau was reached, resulting in six operating conditions (named from A to F), with the dilution rate (D), hydraulic retention time (HRT), and applied OLR consequently derived.

For clarity and comparison, all parameters are reported in Table 1.

Each operating condition was maintained until stable performance in terms of produced current was achieved, and then data were collected. To assess the reproducibility of the proposed screening methodology, the entire experimental protocol (Cases A–F) was repeated for both substrates in a second experimental run using the same MEC reactor,

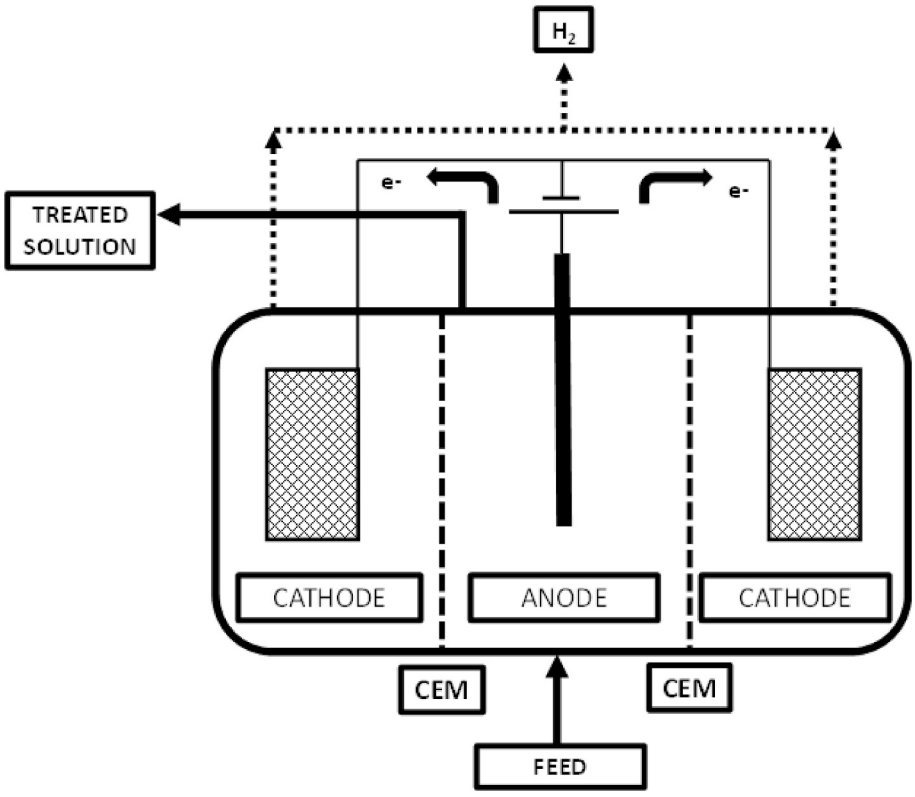

Fig. 1. Schematic illustration of the MEC reactor for hydrogen production, characterized by two abiotic cathodic chamber design. For graphical clarity, the labels 'SYNTH' and 'REAL' are used throughout the figures to denote the synthetic and real substrates, respectively.

Table 1
Operating conditions in terms of flowrate, D rate, HRT and applied OLR for all cases studied.

Case	Q (L/d)	D rate (d^{-1})	HRT (d)	OLR (gCOD/Ld)
A	0.725	0.8	1.2	1.0
B	1.45	1.7	0.6	2.0
C	2.9	3.4	0.3	4.0
D	5.8	6.9	0.15	8.0
E	11.6	13.7	0.07	16.0
F	23.2	27.4	0.04	33.0

resulting in a total of four experimental sets (24 tests overall). Each experimental set lasted approximately 7 days, for a total of 28 days. This approach is intended as repetitions of the experimental protocol rather than independent biological replicates, with the aim to evaluate the repeatability of the proposed screening strategy under consistent reactor configuration and bioanode conditions.

On the other hand, the cathodic chambers were operated in batch mode and filled with a 0.5 M NaCl solution, with daily removal of the catholyte to offset the water electro-osmotic diffusion through the CEM. Additionally, a 0.30 L sampling glass chamber was positioned above each chamber to facilitate the collection of both liquid and gaseous phases. Throughout the entire experimental period, the MEC temperature was maintained at 25 ± 1°C via an external air-conditioning system.

Finally, to monitor and control the potential of individual electrodes, an Ag/AgCl reference electrode (immersed in a saturated KCl solution with $E^{\circ\prime} = 199$ mV vs. the standard hydrogen electrode, SHE) was placed in each MEC chamber. To integrate the graphite granules into the electrical circuit, three graphite rods, serving as collectors, were immersed in the chambers and connected via titanium wires to a potentiostat (IVIUM Technologies, Eindhoven, The Netherlands). A potential of + 0.2 V vs. SHE was applied to the anode, designating it as the working electrode. This anodic value was chosen based on previous findings [46]. For consistency, all voltage measurements reported in this manuscript are referenced against the SHE.

2.2. Real substrate characterization

The fermented solution fed to the MEC reactor was obtained by dark fermentation (DF) of sewage sludge and OFMSW. Sewage sludge was taken from the static thickener connected to the secondary settler of the biological nutrient removal (BNR) water line in the wastewater treatment plant of Treviso (northeast Italy); while food waste was recovered from the source sorted collection of more than 50 districts in the Treviso province and utilized in the DF process after its mechanical trituration, inert removal, squeezing and homogenization. The co-fermentation of sewage sludge and OFMSW was adopted to overcome the seasonal variability and compositional heterogeneity of food waste, while ensuring a continuous supply of organic matter and a more balanced nutrient composition [47]. Indeed, sewage sludge provides a stable and continuously available substrate with buffering capacity, whereas OFMSW contributes readily biodegradable organic compounds, resulting in improved process stability and suitability for biohydrogen-oriented DF [48].

DF process was carried out in a thermophilic stainless steel continuous stirred tank reactor (CSTR) (AISI 304; V 200 L) equipped with a mechanical stirrer and heated by a hot water recirculation system. To maintain the temperature at 55°C, an electrical heater controlled by a PT100-based thermostatic probe was used. Since the CSTR was utilised to maximise hydrogen production, a thermophilic condition was chosen as thermodynamically favourable and slightly affected by the hydrogen partial pressure in the media for this purpose [48]. The CSTR was operated in semi-continuous mode (once per day) and fed with a specific load of 0.2 g zeolite (64% w/w chabazite)/$gVS_{streams}$. Zeolite was added

due to its ion-exchange capacity, high specific surface area, and adsorption properties, which can mitigate potential inhibition by divalent cations and long-chain fatty acids, thereby enhancing hydrogen production during DF. No external inoculum was added, since each test relied on the fermentation capacity of the mixed consortia already present in both streams, according to findings reported elsewhere [48].

The pH was regularly monitored, although no pH-control strategy was adopted, due to the intrinsic buffering capacity provided by sewage sludge. The CSTR was maintained at applied OLR in the range of 12–14 kg VS/(m^3d) and at an HRT of 4 days. Former being supplied to the MEC reactor, the fermentation broth was centrifuged (4700 rpm, Thermo Scientific MEGAFUGE40) and few drops of liquid polyelectrolytes-based flocculant was added to remove suspended solids. After this operation, the fermentation broth was physic-chemical characterised in terms of pH, conductivity, soluble and total chemical oxygen demand, organic acids, alcohol and nutrients content. Values of these components are shown in Table 2.

Nevertheless, the suitability of the fermented effluent as substrate for bioelectrochemical conversion was evaluated considering both its biodegradability and its electrochemical characteristics. The substrate exhibited a high soluble COD fraction (92.4% of the total COD), indicating that most of the organic matter was present in a readily bioavailable form, predominantly composed by organic acids, thereby facilitating microbial uptake and anodic oxidation.

From an electrochemical perspective, the redox potential was used as a valuable indicator of the substrate's intrinsic electron-donating capability. Although the redox potential of complex mixtures cannot be directly determined from the individual compounds, a composition-weighted average redox potential was estimated from the standard redox potentials ($E^{\circ\prime}$) of the main VFAs identified in the fermented effluent, according to the methodology proposed by [49]. The contribution of each compound was weighted according to its relative abundance with respect to the $COD_{soluble}$ fraction. The resulting weighted-average standard redox potential was − 0.249 V vs SHE under standard conditions (pH 7, 25°C, 1 M). Since the fermented substrate exhibited a slightly lower pH than the standard reference conditions, a small positive correction was applied to account for the expected pH-dependent shift in redox potential, resulting in an estimated average value of approximately − 0.278 V vs SHE. This relatively low redox potential reflects the reducing nature of the feedstock, making it particularly suitable as an electron donor. Indeed, when the bioanode is poised at a more positive potential, a favourable thermodynamic gradient is established, promoting efficient electron transfer from the substrate to the electroactive biofilm and supporting sustained current generation and hydrogen evolution at the cathode.

Table 2
Characterization of real effluent obtained from dark fermentation in terms of pH, conductivity, COD soluble and total, ethanol, organic acids and nutrients content.

Real substrate characterization		
pH	5.1 ± 0.3	
σ (mS/cm)	14.4	
		% on COD basis
COD_{total} (g/L)	30.3 ± 3	
$COD_{soluble}$ (g/L)	28.0 ± 3	92.4
Organic acids (gCOD/L)	23 ± 2	82 vs COD_{sol}
EtOH	1.1	4.8
Acetic acid	17.5	76 vs OA
Propionic acid	1.1	5
Butyric acid	3.0	13
Valeric acid	0.7	3
Hexanoic acid	0.7	3
N-NH_4^+ (mg N/L)	625 ± 29	
P-PO_4^{3-} (mg P/L)	77 ± 12	

2.3. Bioanode electro-characterization

Potentiostatic polarization tests were performed by controlling the working electrode potential and recording the resulting current response, allowing electrochemical characterization of the anodic biofilm. This approach helps pinpoint the most energetically favourable and least energy-intensive conditions for conducting the process. The potential was varied of +0.1 stepwise in the range from −0.4 to +0.6 V vs SHE. Each potential step was maintained for at least 2 h to allow current stabilization, and the reported values correspond to the average of the stabilized current signal. This procedure was applied for both synthetic and real substrates and for all investigated operating conditions (cases A–F), enabling determination of the bioanodic kinetics associated with organic matter oxidation. To assess reproducibility, the measurements were performed during duplicated experimental runs, and variability was evaluated based on temporal fluctuations of the stabilized current.

2.4. System characteristic parameters and calculations

To calculate the $COD_{removed}$ (mg/Ld), the following equation was employed, where CODin and CODout (mg/L) represent the influent and effluent COD concentrations, Qin and Qout (L/d) denote the influent and the effluent flow rates, respectively, since in this case are the same, the equation can be further simplified. The result was normalized by the bioanodic chamber volume.

$$COD_{removed}\left(\frac{mg}{Ld}\right) = \frac{Qin*CODin - Qout*CODout}{V} = \frac{Q(CODin - CODout)}{V} \quad (1)$$

From this value was possible to quantify the $COD_{removal}$ efficiency as follows:

$$COD_{removal}efficiency(\%) = \frac{CODremoved}{CODin}*100 \quad (2)$$

The coulombic efficiency (CE), in which meqi represents the cumulative charge that has passed in the circuit and meqCOD represents the cumulative charge generated by the oxidation of the removed COD, was determined according to the equation:

$$CE(\%) = 100*\frac{meqi}{meqCOD} \quad (3)$$

The cathodic coulombic efficiency (CCE) was determined as the ratio of the cumulative H_2 produced, expressed in meq, and the meqi:

$$CCE(\%) = 100*\frac{meqH_2}{meqi} \quad (4)$$

The overall energy efficiency (ηE) was evaluated using the equation:

$$\eta E = \frac{|\Delta G^0 H_2|CCE}{2|\Delta V|F} \quad (5)$$

In which ΔG^0H_2 is the Gibbs free energy for the combustion of hydrogen (kJ/mol), 2 are the mole of electrons necessary to produce a mole of hydrogen (eq/ molH_2), ΔV (V) is the average potential difference between anode and cathode, and F is Faraday's constant (96,485C/eq).

The hydrogen production rate (rH_2) was calculated as follows:

$$rH_2\left(\frac{m^3}{m^3 d}\right) = \frac{d(m^3H_2)}{d(d)}*\frac{1}{V} \quad (6)$$

In which m^3H_2 are cumulative cubic meters of H_2 produced, d corresponds to the days of working period and V is the working reactor volume.

The energetic consumptions (ECH_2) were evaluated as follows:

$$ECH_2\left(\frac{Wh}{Ndm^3H_2}\right) = \frac{24|\Delta V|i}{rH_2 24.4} \quad (7)$$

In which 24 are the hours in a day (h/d), i (A) represents the average electric current registered during the experimental period, rH_2 in mol/d, and 24.4 are the litres (L/ mol) occupied by a mole of gas at a temperature of 25°C.

Importantly, the obtained current generation and $COD_{removal}$ efficiency are represented as a function of D rate (D) for a clearer visualisation of the system response in relation to microbial kinetics:

$$D(d^{-1}) = \frac{Q}{V} = \frac{1}{HRT} \quad (8)$$

In particular, the use of D rate facilitates the graphical identification of system performance plateaus, where further increases in substrate loading or flow rate intensity do not result in proportional gains in electrochemical activity.

2.5. Analytical procedures

The volumetric flow rate of the outlet gas was measured using a Ritter® milligas counter. Gas composition (O_2, H_2, CO_2, and CH_4) was analysed by extracting a 50 μL sample with a gas-tight syringe and injecting into a Dani Master GC gas chromatograph (Milan, Italy) equipped with a thermal conductivity detector (TCD). The COD was assessed by filtering at 0.2 μm and digesting samples at 150°C, using a method reported elsewhere [50]. Conductivity and pH were determined using an SI Analytics HandyLab680 meter (Fisher Scientific, Wien, Austria). The quantification of ethanol and organic acids, present in the real substrate, was conducted using AGILENT 8890 gas chromatograph (GC) equipped with ALS 765A autosampler and a flame ionization detector (FID), maintained at 300°C with air and hydrogen flows of 340 and 30 mL/min respectively. The injector was maintained at 240°C in split mode (10:1). A fused silica capillary column DB-WAX UI Agilent 125-7032UI (30 m x 530 mm × 1.0 μm film thickness) worked under constant hydrogen flow (carrier) of 5.3 mL/min. The chromatographic run was conducted starting from a temperature of 40°C (stable for 1 min) and then increasing it up to 120°C at 10°C/min. The samples were analysed after being centrifuged and filtered with a 0.22 μm filter porosity. Finally, the electrode potentials were manually measured using an Amprobe AM-520-EUR multimeter (Everett, WA, USA). This setup allowed monitoring of the voltage difference (ΔV) between the three compartments of the MEC reactor during operation. Pairwise Student's t-tests were also performed (GraphPad Software, Boston, MA, USA) to compare current production and $COD_{removal}$ efficiencies obtained with synthetic and real substrates under each operating condition. Statistical significance was assumed at $p < 0.05$. Owing to the use of duplicate screening runs performed on the same reactor, these analyses were intended to complement the descriptive statistics rather than to represent fully independent biological comparisons.

3. Results and discussion

3.1. Rapid screening approach to assess the performance of MEC reactor fed with synthetic and real substrates

At the end of the biomass acclimatisation period, to rapidly evaluate the MEC reactor response under different operational conditions and for both tested substrates, the applied flow rate was progressively doubled (D rate increased; HRT decreased). In detail, data collection for each investigated case (A–F) began once stable current values were observed, as current represented the most immediate and continuously monitored performance indicator. Stabilization occurred after approximately three times the HRT for each operating condition, corresponding to 3.5, 1.8, 0.9, 0.5, 0.2, and 0.1 days (85, 43, 21, 11, 5, and 3 h) for cases A to F, respectively, consistent with biological systems steady-state evolution, as reported in [51]. After stabilization, the daily current was averaged, and liquid and gas analyses were performed. The reported values correspond to the mean of two experimental set for each substrate, as explained in "*2. Material and Methods*". Average trends of current and $COD_{removal}$ efficiency are reported in Fig. 2**.A** and Fig. 2**.B**. Corresponding figures based on HRT parameter are shown in Supplementary Material (Figs. S.1.A and S.1.B).

In Fig. 2.A, the observed current increased with the increase of D rate, indicating enhanced electroactive performance at higher flow rates. In contrast, Fig. 2.B reveals an opposite trend for $COD_{removal}$ efficiency, which decreased when the D rate rose. This inverse relationship suggested a trade-off between system productivity, in terms of electrochemical activity and organic matter removal, with faster flow rates favouring electron transfer but limiting substrate degradation.

Indeed, the highest current production was observed in case F, reaching 170 ± 4 and 157 ± 5 mA for the synthetic and real substrates, respectively, but exhibiting the lowest COD removal performance, with $COD_{removed}$ around 3.8 and 3.6 gCOD/Ld, corresponding to a removal efficiency of 12 ± 1.5% and 11 ± 1%, respectively. Conversely, the maximum $COD_{removal}$ efficiencies (64 ± 1.5% and 39 ± 2%) were achieved in case A, where 0.65 and 0.37 gCOD/Ld were removed associated with the lowest current production, of 44 ± 1 and 37 ± 1 mA, for the synthetic and real substrates, respectively.

Moreover, the transition from condition E to F resulted in only a marginal increase in current production (percentage deviation approximately 5%), while no appreciable variation was observed in $COD_{removal}$ efficiency, clearly indicating that the system reached a plateau region. Thus, further intensification of hydraulic conditions does not translate into additional significant electrochemical or treatment benefits. The statistical analysis (Table S2) further supported the progressive convergence between synthetic and real substrates. Significant differences in current production were only observed under the lowest hydraulic conditions (Cases A and B, $p < 0.05$), whereas no statistically significant differences were observed at the highest hydraulic conditions (Cases D–F, $p > 0.05$), supporting the progressive convergence of reactor performance discussed above. A similar trend was observed for COD removal efficiency.

Hence, identifying the onset of the performance plateau enables a more informed selection of operating conditions for subsequent long-term studies. Rather than investing time and resources in steady-state experiments under hydraulically intensified conditions, yielding only marginal performance improvements, the proposed screening allows detailed investigations to focus on the most relevant operating window according to the desired process objective.

Although no intrinsic kinetic parameters were derived in the present study, the observed performance plateau exhibited a saturation-type behaviour that is consistent with the substrate consumption trends commonly described for attached-growth systems [51], also compatible with the progressive reduction of external mass-transfer limitations typically described for packed-bed bioreactors with immobilized biomass, as discussed by Doran [52]. At low D rates, substrate transport towards the biofilm may limit the overall reaction rate, whereas increasing the flow rate enhances convective transport, progressively reducing these limitations. Beyond a certain hydraulic condition further increases in flow rate no longer produce substantial gains in current, suggesting that the system approaches a saturation regime in which intrinsic biological processes become increasingly dominant. At the same time, increasing the D rate inevitably shortens the hydraulic retention time, reducing the contact time available for substrate conversion. Consequently, although higher substrate availability supports increased current production, $COD_{removal}$ efficiency progressively decreases. Consequently, MEC performance reflects a balance between substrate availability, HRT, substrate conversion efficiency and electrochemical response.

Fig. 3.A reports a comparative overview of the main performance

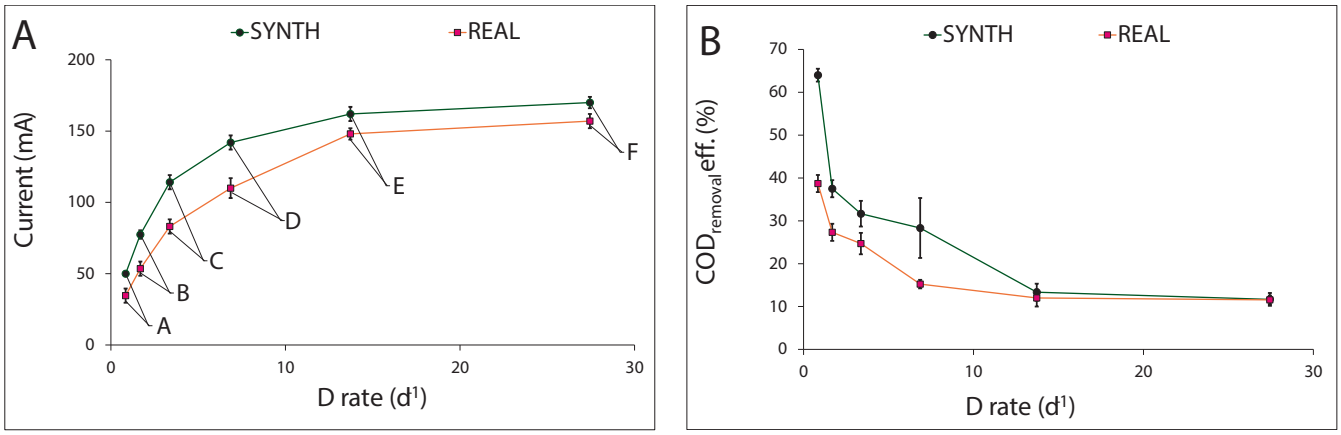

Fig. 2. Trends of the produced cathodic current (A) and of $COD_{removal}$ efficiency obtained (B) in MEC reactor as a function of D rate for all operating conditions, for both synthetic and real substrates.

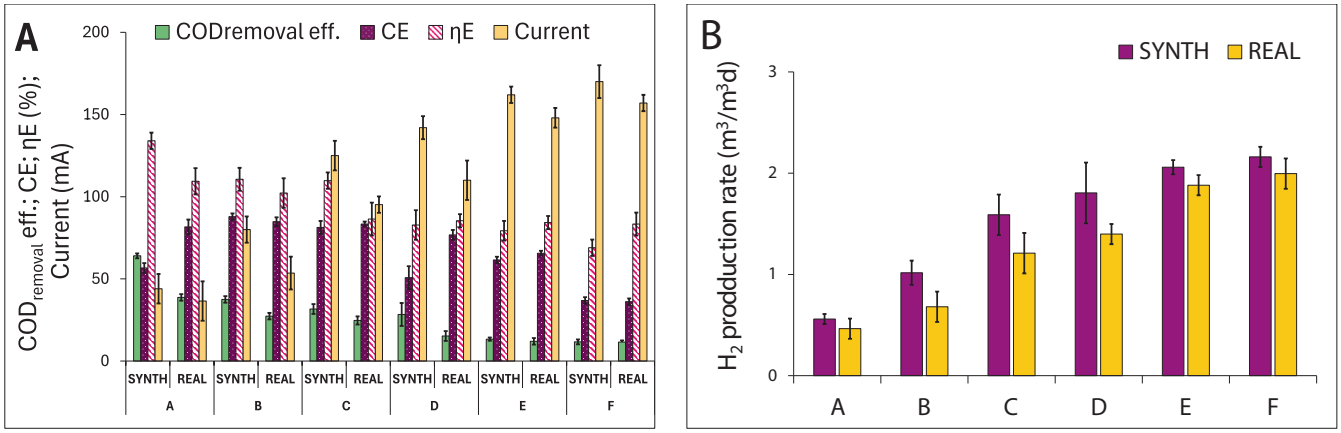

Fig. 3. Trends of the main characterizing parameters of the MEC system (A) and of the H_2 production rates (B) obtained for all operating conditions, for both synthetic and real substrates.

indicators averaged between the two experimental setups for the MEC system, for synthetic and real substrates. The parameters include $COD_{removal}$ efficiency, current intensity, coulombic and overall energy efficiencies. Moreover, gas-phase characterizations, including daily volumetric gas flow and composition, permitted to obtain information about the H_2 production rate for all cases, reported in Fig. 3.B, and further established that hydrogen was the sole gaseous product formed in all tested conditions.

Notably, in all experimental conditions, the cathodic chamber pH spontaneously reached approximately a value of 13; a strongly alkaline environment that effectively inhibits most hydrogenophilic microbial metabolisms. The observed pH value was a direct consequence beyond the chosen catholyte, as the NaCl solution is characterised by a lack of buffering capacity, which favoured alkalinization of the cathodic chamber. Indeed, the migration of cations such as Ca^{2+}, Mg^{2+}, K^{+}, and Na^{+}, from the anode to the cathode, through the CEM to maintain electroneutrality promoted the continuous alkalinity generation in the cathodic chamber, which limited acetate generation and suppressed completely methanogenesis pathways, shifting the consumption of equivalents in a highly selective and efficient hydrogen production [53,54].

Indeed, no methane was detected, most notably the CCE consistently ranged between 96 and 100% across all tested conditions, confirming that almost all the electrons reaching the cathode were effectively converted into hydrogen. Although minor gas losses during sampling or collection cannot be entirely excluded, these would result in a slight underestimation rather than an overestimation of the calculated CCE, further supporting the effectiveness of the dual-cathode configuration.

As shown in the Fig. 3.A, current intensity progressively increased with the flow rate increment, for both substrates peaking at 198 ± 5 A/m^3 (synthetic) and 183 ± 6 A/m^3 (real) in case F. This is also mirrored in the Fig. 3.B trend, with a maximum of H_2 production rate reached for case F equal to 2.2 ± 0.1 and 2.0 ± 0.15 m^3/ m^3 d for synthetic and real substrates, respectively. This reflects the improved electron production at higher substrate loadings. However, this is attended by a significant decline in $COD_{removal}$ efficiency and CE, especially under high-flow rate conditions, with minimum values of CE equal to 36–37% observed in case F, consistent with previous observations (Fig. 2.B). Interestingly, cases E and F yielded very similar values for CE and $COD_{removal}$ efficiency, but in case F a slight drop in the latter was observed, suggesting the onset of kinetic or transport limitations. Once again, these results clearly reflect the limitations imposed by metabolic saturation and a high feed rate for effective substrate assimilation.

In **Table S2** a synthesis of the average data of MEC system's performance parameters under all tested conditions are shown.

Overall, the synthetic substrate systematically outperformed the real one, particularly in early cases (A–C). This behaviour is to be attributed to the simpler and more readily biodegradable nature of the synthetic feedstock, which facilitated faster microbial metabolism compared to the real substrate, characterised by a more complex composition. In addition, part of the performance difference between the two substrates can also be attributed to their different conductivities, a more detailed discussion of this influence on the electrochemical response is provided in "*Section 3.2. Bioanode electro-characterization*". Nevertheless, both

substrates enabled stable hydrogen production with high energy efficiency across all tested conditions, demonstrating also comparable performance in terms of CCE and current production at higher flow rates, indicating the robustness of the microbial consortia even under stress.

Looking ahead, the proposed screening strategy can serve as a practical decision-support tool, providing a robust and efficient framework for the rapid identification of performance trends and operational boundaries in MEC systems. Rather than performing a comprehensive electrochemical and biological characterization under every investigated operating condition, this preliminary assessment enables the rapid exclusion of suboptimal scenarios and the selection of the most promising operating windows for subsequent long-term investigations. Consequently, experimental efforts can be focused on a limited number of conditions, reducing both experimental time and resource consumption while maintaining reliable process evaluation.

Furthermore, by rapidly assessing the effects of hydraulic conditions and OLR on both anodic and cathodic performance, the proposed approach facilitates the optimisation of MECs towards specific objectives, including biohydrogen production, wastewater treatment, or a balanced compromise between cathodic and anodic targets. From an operational perspective, lower hydraulic loading conditions favour $COD_{removal}$ efficiency, whereas higher loading rates enhance current generation and hydrogen production. Consequently, the proposed screening enables the identification of the most appropriate operating window according to the desired process objective, while minimizing the risks of biomass wash-out, microbial overloading, and unnecessary long-term operation under suboptimal conditions.

3.2. Bioanode electro-characterization

In support of the screening test, further investigation was done through electro-characterization of the bioanode. Indeed, electroanalytical techniques are powerful tools for investigating the electrochemical response of microbial bioelectrodes, providing important information on the bioanode behaviour. Nevertheless, their application is often challenged by the complex and dynamic nature of the biofilm–electrode interface [55].

The current produced at the bioanode as a function of the applied anodic potential (vs SHE) are shown in Fig. 4, where the average anodic kinetic curves obtained under steady-state conditions for all cases examined in duplicate, and for both synthetic and real substrates, are reported. However, the observed deviations were negligible and therefore not visible at the scale of the reported curves.

First, in all cases, a clear inhibition of biological activity is observed at anodic potentials below –0.1 V vs SHE for both substrates. This behaviour can be attributed to the lower energy level imposed on the granular graphite, acting as the terminal electron acceptor. Under such low-potential conditions, the electron transfer from the microbial electron transport chain to the electrode becomes thermodynamically unfavourable, thus resulting in a progressive decrease in current generation. Second, at anodic potentials above + 0.2 V vs SHE, the current plateaus were reached for all cases, indicating that further increases in potential no longer significantly enhance electron transfer. Although a slight increase in current is observed at higher potentials, it does not justify the additional energy input required, which would compromise the energy balance of the process.

It is also worth noting that, a systematic increase in current density was observed when the synthetic substrate was used, compared to the real fermented feedstock, across all investigated operating conditions. At the highest applied anode potential (+ 0.6 V vs SHE), the relative increment in current production reached approximately 41% in Case A and remained close to 30% in Cases B–D, while a markedly lower difference (≈12%) was recorded in Cases E and F. This discrepancy can be primarily attributed to the lower electrolyte conductivity of the diluted real substrate (2.0 real vs 6.0 synthetic mS/cm), resulting in a higher internal resistance limiting the electron flow and current output of the system. According to Ohm's law for electrolytic solutions, electrical resistance is inversely proportional to electrolyte conductivity. Therefore, the lower conductivity of the real substrate results in greater ohmic losses, which become increasingly significant at higher anode potentials, where internal resistance exerts a stronger influence on the electrochemical response. Consequently, a higher potential difference was required to sustain the same current flow, contributing to the lower overall energy efficiency observed when the real substrate was fed to the reactor.

However, the progressive reduction in the relative current enhancement observed at increasing flow rate suggests a shift in the dominant limiting mechanisms. Indeed, under higher operating conditions, anodic performance is likely governed by substrate transport

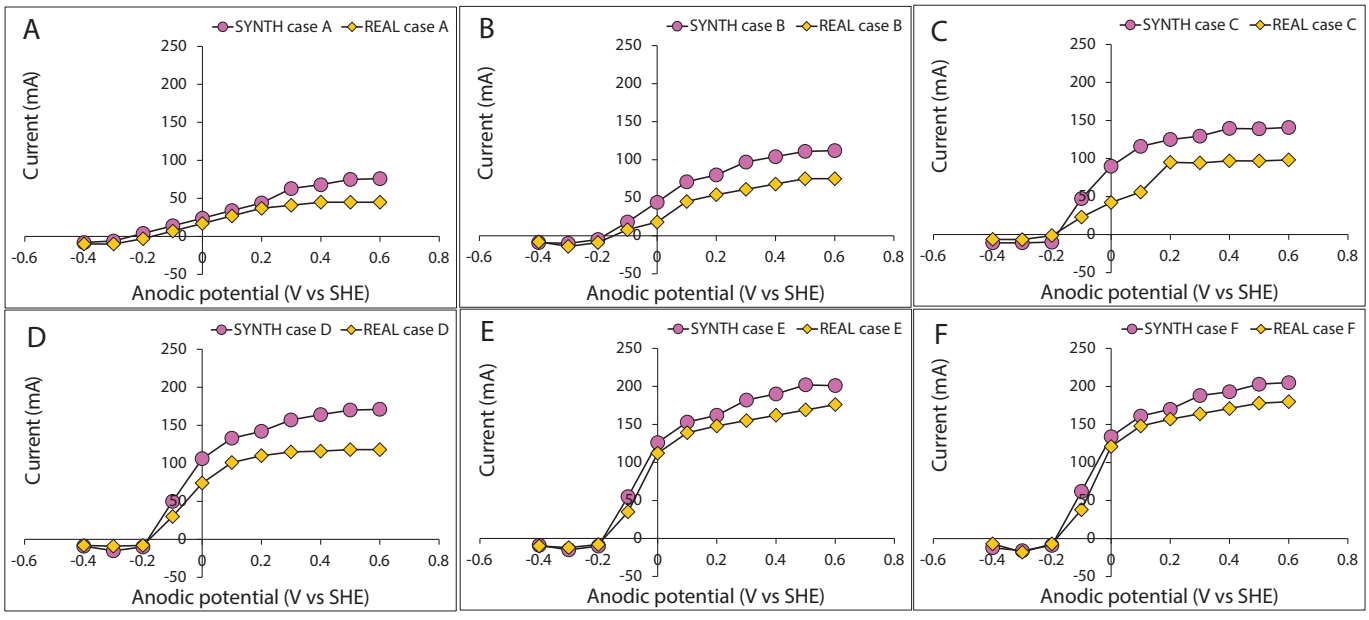

Fig. 4. Electrochemical characterization by potentiostatic technique: bioanodic kinetic curves obtained for synthetic and real substrates under all operating conditions (A–F). Current values correspond to stabilized responses at each applied potential.

phenomena and bioelectrochemical constraints, such as metabolic saturation, charge transfer limitations, or microbial stress, rather than by purely ohmic resistance. Consequently, the advantage associated with the higher conductivity of the synthetic substrate becomes less significant, leading to a near convergence of current production between synthetic and real feedstocks.

Overall, these kinetic results provide a valuable basis for defining the optimal anodic potential window for MEC operation under potentiostatic control. In particular, the applied anodic potential of + 0.2 V vs SHE adopted in this study appears to provide a favourable compromise between efficient electron transfer and minimising the external energy input required to sustain the process. Since external power demand remains one of the main factors limiting the large-scale implementation of MEC technology, the identification of energy-efficient operating conditions represents a key step towards improving the overall sustainability and practical feasibility of bioelectrochemical hydrogen production. Combined with the proposed rapid screening strategy, this electrochemical characterization provides practical guidelines for selecting operating conditions that maximize reactor performance while limiting unnecessary energy consumption, thereby supporting more sustainable MEC operation.

3.3. Performance comparison between dual- and single-cathode MEC design

A comparative analysis with selected literature studies was performed by focusing on MEC systems operating under comparable OLR and HRT, to isolate the effect of reactor design on electrochemical performance. The present work was benchmarked against Zeppilli et al. (2017) [44] and Marchetti et al. (2025) [45], which share the same reactor geometry, electrode materials, membrane type (CEM) and whose bioanodes were inoculated with sludge from the same wastewater treatment plant, thus providing a highly consistent experimental and anodic framework for engineering comparison. Although minor differences associated with biofilm development and biological adaptation cannot be completely excluded, these studies represent the most suitable benchmark currently available for evaluating the potential influence of the dual-cathode configuration ensuring a meaningful performance assessment. The main operational and performance parameters for both synthetic and real substrates are summarised in Table 3.

A direct comparison of the obtained results, for case B, was made with the system of Zeppilli et al., fed with an effluent coming from two-phase anaerobic digestion, operated at the same HRT, applied potential and very similar OLR. While a slightly higher current density (≈63 A/m^3) was obtained in the present study with the real substrate, near complete recovery of the generated current as hydrogen (CCE ≈ 100%) was achieved, compared to 51% reported by Zeppilli et al. In this latter, the CE values exceeding 100% were attributed to the underestimation of soluble COD due to slowly hydrolysable particulate matter, as noted by the authors during the reactor working period, thus overestimating the CE calculation.

Similar advantages were observed when comparing Marchetti et al., (2025) with the results of case C, conducted at the same OLR and HRT. It shown that despite the higher anodic potential applied in that study (+0.3 V vs SHE), the achieved current density was lower than that obtained here with the synthetic substrate and comparable with the real feed. This corresponds to an improvement of 46.5% and 11.1% in current density for synthetic and real substrates, respectively, which can be attributed to the dual-cathode design. The performance improvement is supported also by higher CE here obtained, indicating more effective electron recovery per unit of COD oxidised, corresponding to an increment of 21% and 24% for synthetic and real substrate, respectively, as well as consistently higher CCE and overall energy ηE (+ 32.5% and + 3.6%, respectively) compared to the single-cathode system. Hydrogen productivity was comparable but achieved at a substantially lower energy cost in the present study (2.9 vs 6.32 kWh/Nm^3H_2), in line with the lower electrode potential difference (ΔV = 1.35 vs 2.64 V), when synthetic feed was used. While, when operating with real fermented feedstock, owing to a similarly elevated ΔV (2.56 V), the energetic consumption obtained (6.7 kWh/Nm^3H_2) closely matched with that reported by Marchetti et al. (2025).

While acknowledging that additional operational and biological factors also influence reactor performance, overall, these results indicate that the dual-cathode configuration contributes for enhancing the electrochemical performance of the MEC system.

4. Conclusions

This study introduced a rapid screening approach for the systematic evaluation of MEC performance under varying hydraulic conditions, enabling the sequential exploration of multiple operating points. Rather than replacing conventional long-term MEC optimisation process, the proposed strategy serves as a preliminary diagnostic tool that rapidly narrows the operational window before detailed system characterization. Indeed, the variation of hydraulic operating conditions revealed a clear trade-off between current and hydrogen production and $COD_{removal}$ efficiency, allowing rapid identification of the performance plateaus. For both substrates, the plateau observed at dilution factors ≥11.6 d^{-1} indicated a common operational limitation, accompanied by a progressive decline in anodic coulombic efficiency. Complementary bioelectrochemical characterization provided mechanistic insight into these performance trends, suggesting that under higher hydraulic loading conditions substrate transport limitations were likely the predominant limiting factor rather than electrode kinetics. In addition, the dual-cathode configuration also contributed to enhance electrochemical performance (CCE ≈ 100% for all cases), compared with similar single-cathode systems reported in the literature. Although duplicate experiments confirmed the reproducibility of the proposed screening methodology, future studies employing independent reactor replicates and long-term continuous operation will further strengthen its biological robustness and applicability. Overall, beyond the specific reactor configuration investigated in this study, the proposed rapid screening approach provides a practical framework for the early-stage evaluation of MEC systems, may facilitating the development, optimization, and future scale-up of bioelectrochemical technologies for hydrogen production and waste valorisation.

Table 3
Comparison of dual-cathode MEC performance obtained in this work with single-cathode literature studies in terms of the main characteristic parameters.

Ref. study	Feed type	OLR (gCOD/Ld) HRT (d)	Current density (A/m^3)	$COD_{removal}$ efficiency (%)	CE (%)	CCE (%)	ηE (%)	H_2 prod. rate (m^3/m^3d)
This study Case B	Synthetic	2.0; 0.6	93 ± 9	38 ± 2	88 ± 2	≈ 100	111 ± 7	1.0
	Real		63 ± 12	27 ± 2	85 ± 3	≈ 100	102 ± 9	0.7
[44][a]	Real	1.5; 0.6	60 ± 4	28 ± 3	119 ± 28	51 ± 1	–	–
This study Case C	Synthetic	4.0; 0.3	145 ± 10	32 ± 3	81 ± 4	≈ 100	110 ± 5	1.6
	Real		110 ± 10	25 ± 2	83 ± 1	≈ 100	86 ± 10	1.2
[45][b]	Synthetic	4.0; 0.3	99 ± 2	42 ± 1	67 ± 1	74 ± 1	83 ± 1	1.3

[a] Reactor, with the methane production target, fed with a mix of anaerobic digestate and acidogenic fermented coming from OFMSW treatment plant.
[b] Working potential set to + 0.3 V vs SHE.

CRediT authorship contribution statement

Angela Marchetti: Writing – original draft, Methodology, Investigation, Formal analysis, Data curation, Conceptualization. **Francesco Valentino:** Writing – review & editing, Methodology, Formal analysis. **Marco Gottardo:** Methodology, Formal analysis. **Marco Zeppilli:** Writing – review & editing, Validation, Supervision, Project administration, Methodology, Investigation, Funding acquisition, Conceptualization.

Declaration of competing interest

The authors declare that they have no known competing financial interests or personal relationships that could have appeared to influence the work reported in this paper.

Acknowledgements

The authors gratefully acknowledge the Italian National Institute for Insurance against Accidents at Work (Istituto Nazionale per l'Assicurazione contro gli Infortuni sul Lavoro, INAIL) for financial support of this research, in the frame of national Call BRiC 2022, Piano Attività di Ricerca 2022/2024, (ID64). This work was conducted as part of the HUMANFORHYDRO project (20223W9KPM), funded under the framework of PRIN 2022 Call.

Appendix A. Supplementary data

Supplementary data to this article can be found online at https://doi.org/10.1016/j.seta.2026.105351.

Data availability

Data will be made available on request.

References

[1] Filonchyk M, Peterson MP, Zhang L, Hurynovich V, He Y. Greenhouse gases emissions and global climate change: Examining the influence of CO2, CH4, and N2O. Sci Total Environ 2024;935:173359. https://doi.org/10.1016/J.SCITOTENV.2024.173359.
[2] Senthil Rathi B, Senthil Kumar P, Rangasamy G, Rajendran S. A critical review on Biohydrogen generation from biomass. Int J Hydrogen Energy 2024;52:115–38. https://doi.org/10.1016/j.ijhydene.2022.10.182.
[3] Chataut G, Bhatta B, Joshi D, Subedi K, Kafle K. Greenhouse gases emission from agricultural soil: a review. J Agric Food Res 2023;11:100533. https://doi.org/10.1016/J.JAFR.2023.100533.
[4] Marchetti A, Lorini L, Salvatori G, Gianico A, Majone M, Villano M. Polyhydroxyalkanoates production by mixed microbial cultures in sequencing batch reactors operated under different feeding conditions. Chem Eng Trans 2022;93:163–8. https://doi.org/10.3303/CET2293028.
[5] Wolf S, Teitge J, Mielke J, Schütze F, Jaeger C. The European green deal — more than climate neutrality. Intereconomics 2021;56:99–107. https://doi.org/10.1007/S10272-021-0963-Z/METRICS.
[6] Mneimneh F, Ghazzawi H, Abu Hejjeh M, Manganelli M, Ramakrishna S. Roadmap to achieving sustainable development via green hydrogen. Energies 2023;16:1368. https://doi.org/10.3390/EN16031368.
[7] Shiva Kumar S, Lim H. An overview of water electrolysis technologies for green hydrogen production. Energy Rep 2022;8:13793–813. https://doi.org/10.1016/J.EGYR.2022.10.127.
[8] Holladay JD, Hu J, King DL, Wang Y. An overview of hydrogen production technologies. Catal Today 2009;139:244–60. https://doi.org/10.1016/J.CATTOD.2008.08.039.
[9] Nikolaidis P, Poullikkas A. A comparative overview of hydrogen production processes. Renew Sustain Energy Rev 2017;67:597–611. https://doi.org/10.1016/J.RSER.2016.09.044.
[10] Yu M, Wang K, Vredenburg H. Insights into low-carbon hydrogen production methods: Green, blue and aqua hydrogen. Int J Hydrogen Energy 2021;46:21261–73. https://doi.org/10.1016/J.IJHYDENE.2021.04.016.
[11] Zainal BS, Ker PJ, Mohamed H, Ong HC, Fattah IMR, Rahman SMA, et al. Recent advancement and assessment of green hydrogen production technologies. Renew Sustain Energy Rev 2024;189:113941. https://doi.org/10.1016/J.RSER.2023.113941.
[12] Saravanan A, Karishma S, Kumar PS, Yaashikaa PR, Jeevanantham S, Gayathri B. Microbial electrolysis cells and microbial fuel cells for biohydrogen production: current advances and emerging challenges. Biomass Conver. Bioref. 2020;13:8403–23. https://doi.org/10.1007/S13399-020-00973-X.
[13] Marchetti A, Palhas M, Villano M, Fradinho J. Valorization of reground pasta by-product through PHA production with phototrophic purple bacteria. Catalysts 2024;14:239. https://doi.org/10.3390/catal14040239.
[14] Hussien M, Mohamed HO, Jadhav DA, Bahaa A, Jo SM, Jang JH, et al. Synergistic integration of dark fermentation and microbial electrolysis cells for hydrogen production and sustainable swine manure treatment. Int J Hydrogen Energy 2025;115:299–309. https://doi.org/10.1016/J.IJHYDENE.2025.02.453.
[15] Marchetti A, Palhas M, Villano M, Reis MAM, Fradinho J. Unlocking the potential of food industry by-products: Sustainable volatile fatty acids production via mixed culture acidogenic fermentation of reground pasta. J Clean Prod 2025;526:146633. https://doi.org/10.1016/j.jclepro.2025.146633.
[16] Bora A, Mohanrasu K, Angelin Swetha T, Ananthi V, Sindhu R, Chi NTL, et al. Microbial electrolysis cell (MEC): Reactor configurations, recent advances and strategies in biohydrogen production. Fuel 2022;328. https://doi.org/10.1016/j.fuel.2022.125269.
[17] Savla N, Guin M, Pandit S, Malik H, Khilari S, Mathuriya AS, et al. Recent advancements in the cathodic catalyst for the hydrogen evolution reaction in microbial electrolytic cells. Int J Hydrogen Energy 2022;47:15333–56. https://doi.org/10.1016/J.IJHYDENE.2022.03.058.
[18] Marchetti A, Sassetto G, Cabras D, Hosseini S, Milia S, Zeppilli M. From wastewater to bio-hydrogen: advancing microbial electrolysis cells through challenges, innovations, and process integration. Hydrogen 2026;7:85. https://doi.org/10.3390/hydrogen7020085.
[19] Khandaker S, Das S, Hossain MT, Islam A, Miah MR, Awual MR. Sustainable approach for wastewater treatment using microbial fuel cells and green energy generation – a comprehensive review. J Mol Liq 2021;344:117795. https://doi.org/10.1016/J.MOLLIQ.2021.117795.
[20] Arun J, SundarRajan PS, Grace Pavithra K, Priyadharsini P, Shyam S, Goutham R, et al. New insights into microbial electrolysis cells (MEC) and microbial fuel cells (MFC) for simultaneous wastewater treatment and green fuel (hydrogen) generation. Fuel 2024;355:129530. https://doi.org/10.1016/J.FUEL.2023.129530.
[21] Roubaud E, Lacroix R, Da Silva S, Bergel A, Basséguy R, Erable B. Catalysis of the hydrogen evolution reaction by hydrogen carbonate to decrease the voltage of microbial electrolysis cell fed with domestic wastewater. Electrochim Acta 2018;275:32–9. https://doi.org/10.1016/j.electacta.2018.04.135.
[22] Sergienko N, Irtem E, Gutierrez O, Radjenovic J. Electrochemical removal of sulfide on porous carbon-based flow-through electrodes. J Hazard Mater 2019;375:19–25. https://doi.org/10.1016/j.jhazmat.2019.04.033.
[23] Ruiz Y, Baeza JA, Guisasola A. Microbial electrolysis cell performance using non-buffered and low conductivity wastewaters. Chem Eng J 2016;289:341–8. https://doi.org/10.1016/J.CEJ.2015.12.098.
[24] Wang YZ, Zhang L, Xu T, Ding K. Influence of initial anolyte pH and temperature on hydrogen production through simultaneous saccharification and fermentation of lignocellulose in microbial electrolysis cell. Int J Hydrogen Energy 2017;42:22663–70. https://doi.org/10.1016/J.IJHYDENE.2017.07.214.
[25] Shao Q, Li J, Yang S, Sun H. Effects of different substrates on microbial electrolysis cell (MEC) anodic membrane: biodiversity and hydrogen production performance. Water Sci Technol 2019;79:1123–33. https://doi.org/10.2166/WST.2019.107.
[26] Matturro B, Zeppilli M, Lai A, Majone M, Rossetti S. Metagenomic Analysis reveals Microbial Interactions at the Biocathode of a Bioelectrochemical System Capable of Simultaneous Trichloroethylene and Cr(VI) Reduction. Front Microbiol 2021;12:747670. https://doi.org/10.3389/FMICB.2021.747670/XML.
[27] Islam AK. Hydropower coupled with hydrogen production from wastewater: Integration of micro-hydropower plant (MHP) and microbial electrolysis cell (MEC). Int J Hydrogen Energy 2024;49:1–14. https://doi.org/10.1016/J.IJHYDENE.2023.06.179.
[28] Khan MZ, Nizami AS, Rehan M, Ouda OKM, Sultana S, Ismail IM, et al. Microbial electrolysis cells for hydrogen production and urban wastewater treatment: a case study of Saudi Arabia. Appl Energy 2017;185:410–20. https://doi.org/10.1016/J.APENERGY.2016.11.005.
[29] Kundu A, Narayan Sahu J, Redzwan G, Hashim MA. An overview of cathode material and catalysts suitable for generating hydrogen in microbial electrolysis cell 2012. 10.1016/j.ijhydene.2012.11.031.
[30] Lee HS, Torres CI, Parameswaran P, Rittmann BE. Fate of H2 in an upflow single-chamber microbial electrolysis cell using a metal-catalyst-free cathode. Environ Sci Technol 2009;43:7971–6. https://doi.org/10.1021/es900204j.
[31] Sangeetha T, Guo Z, Liu W, Cui M, Yang C, Wang L, et al. Cathode material as an influencing factor on beer wastewater treatment and methane production in a novel integrated upflow microbial electrolysis cell (Upflow-MEC). Int J Hydrogen Energy 2016;41:2189–96. https://doi.org/10.1016/J.IJHYDENE.2015.11.111.
[32] Bora A, Mohanrasu K, Angelin Swetha T, Ananthi V, Sindhu R, Chi NTL, et al. Microbial electrolysis cell (MEC): Reactor configurations, recent advances and strategies in biohydrogen production. Fuel 2022;328:125269. https://doi.org/10.1016/J.FUEL.2022.125269.
[33] Liu Z, Xue X, Cai W, Cui K, Patil SA, Guo K. Recent progress on microbial electrosynthesis reactor designs and strategies to enhance the reactor performance. Biochem Eng J 2023;190:108745. https://doi.org/10.1016/J.BEJ.2022.108745.
[34] Ghalloussi R, Garcia-Vasquez W, Bellakhal N, Larchet C, Dammak L, Huguet P, et al. Ageing of ion-exchange membranes used in electrodialysis: Investigation of static parameters, electrolyte permeability and tensile strength. Sep Purif Technol 2011;80:270–5. https://doi.org/10.1016/J.SEPPUR.2011.05.005.
[35] DuChanois RM, Mazurowski L, Fan H, Verduzco R, Nir O, Elimelech M. Precise cation separations with composite cation-exchange membranes: role of base layer

properties. Environ Sci Technol 2023;57:6331–41. https://doi.org/10.1021/ACS.EST.3C00445/ASSET/IMAGES/LARGE/ES3C00445_0004.JPEG.
[36] Stoller M, Marchetti A, Ochando Pulido JM. On the effect of specific boundary flux parameters on membrane process design. Chem Eng Trans 2019;74. https://doi.org/10.3303/CET1974115.
[37] Alcaraz-Gonzalez V, Flores-Estrella RA, Nolasco M, Cano V, González-Alvarez V. Microbial Electrolysis Cells for Biohydrogen Generation and Wastewater Treatment—A Short Review and Current Trends 2023:73–85. https://doi.org/10.1007/978-3-031-36298-9_6.
[38] Kanellos G, Tremouli A, Arvanitakis G, Lyberatos G. Boosting methane production and raw waste activated sludge treatment in a microbial electrolysis cell-anaerobic digestion (MEC-AD) system: the effect of organic loading rate. Bioelectrochemistry 2024;155:108555. https://doi.org/10.1016/J.BIOELECHEM.2023.108555.
[39] Sharma A, Hussain Mehdi SE, Pandit S, Eun-Oh S, Natarajan V. Factors affecting hydrogen production in microbial electrolysis cell (MEC): a review. Int J Hydrogen Energy 2024;61:1473–84. https://doi.org/10.1016/J.IJHYDENE.2024.02.193.
[40] Jadhav DA, Kumar G, Jang JK, Chae KJ. Biohydrogen upgradation and wastewater treatment in 3-chambered bioelectrochemical system assisted with H2/O2-based redox reactions. J Environ Manage 2024;368:122209. https://doi.org/10.1016/J.JENVMAN.2024.122209.
[41] Mah RA, Smith MR. The Methanogenic Bacteria. The Prokaryotes 1981:948–77. https://doi.org/10.1007/978-3-662-13187-9_76.
[42] Balch WE, Fox GE, Magrum LJ, Woese CR, Wolfe RS. Methanogens: reevaluation of a unique biological group. Microbiol Rev 1979;43:260–96. https://doi.org/10.1128/MR.43.2.260-296.1979.
[43] Zeppilli M, Paiano P, Villano M, Majone M. Anodic vs cathodic potentiostatic control of a methane producing microbial electrolysis cell aimed at biogas upgrading 2019. https://doi.org/10.1016/j.bej.2019.107393.
[44] Zeppilli M, Pavesi D, Gottardo M, Micolucci F, Villano M, Majone M. Using effluents from two-phase anaerobic digestion to feed a methane-producing microbial electrolysis. Chem Eng J 2017;328:428–33. https://doi.org/10.1016/J.CEJ.2017.07.057.
[45] Marchetti A, Cerrillo Moreno M, Lauri R, Zeppilli M. Optimizing hydrogen production through efficient organic matter oxidation performed by microbial electrolysis cells. Processes 2025;13:1231. https://doi.org/10.3390/pr13041231.
[46] Cerrillo M, Viñas M, Bonmatí A. Removal of volatile fatty acids and ammonia recovery from unstable anaerobic digesters with a microbial electrolysis cell. Bioresour Technol 2016;219:348–56. https://doi.org/10.1016/J.BIORTECH.2016.07.103.
[47] Vidal-Antich C, Perez-Esteban N, Astals S, Peces M, Mata-Alvarez J, Dosta J. Assessing the potential of waste activated sludge and food waste co-fermentation for carboxylic acids production. Sci Total Environ 2021;757:143763. https://doi.org/10.1016/J.SCITOTENV.2020.143763.
[48] Gottardo M, Khorramian N, Pavan P, Battista F, Bolzonella D, Lauri R, et al. Assessment of the hydrogen production potential in a zeolite assisted two-phase dark and photo-fermentation process from urban waste mixture. Resources 2025;14:43. https://doi.org/10.3390/RESOURCES14030043.
[49] Freguia S, Teh EH, Boon N, Leung KM, Keller J, Rabaey K. Microbial fuel cells operating on mixed fatty acids. Bioresour Technol 2010;101:1233–8. https://doi.org/10.1016/J.BIORTECH.2009.09.054.
[50] Marchetti A, Berhouma S, Chouchane H, Zeppilli M. Brewery wastewater treatment coupled to green hydrogen production through microbial electrolysis cell. Chem Eng Trans 2026;124:343–8. https://doi.org/10.3303/CET26124058.
[51] Hamelers HVM, ter Heijne A, Stein N, Rozendal RA, Buisman CJN. Butler–Volmer–Monod model for describing bio-anode polarization curves. Bioresour Technol 2011;102:381–7. https://doi.org/10.1016/J.BIORTECH.2010.06.156.
[52] Doran PM. Bioprocess Engineering Principles. 1st ed. Elsevier Science; 1995. https://doi.org/https://books.google.it/books?hl=it&lr=&id=GoOqw3hKIyIC&oi=fnd&pg=PP1&dq=bioprocess+engineering+principles+pauline&ots=ZO3aks9keW&sig=EuGoIWIDYyjEHBty210-dLAJxFM&redir_esc=y#v=onepage&q=bioprocess%20engineering%20principles%20pauline&f=false.
[53] Wainaina S, Lukitawesa, Kumar Awasthi M, Taherzadeh MJ. Bioengineering of anaerobic digestion for volatile fatty acids, hydrogen or methane production: a critical review. Bioengineered 2019;10:437–58. https://doi.org/10.1080/21655979.2019.1673937.
[54] Laiq Ur Rehman M, Iqbal A, Chang C, Li W, Ju M. Anaerobic digestion. Water Environ Res 2019;91:1253–71. https://doi.org/10.1002/wer.1219.
[55] Segundo-Aguilar A, Trejo G, Rivero EP, Rivera FF, Cercado B. Bioelectrochemical characterization of a biogas-producing microbial electrolysis cell (MEC): advantages and limitations of electroanalytical techniques. Bioelectrochemistry 2026;168:109128. https://doi.org/10.1016/J.BIOELECHEM.2025.109128.